

## Tuning Density Profiles and Mobility of Inhomogeneous Fluids

Gaurav Goel,<sup>1</sup> William P. Krekelberg,<sup>1</sup> Jeffrey R. Errington,<sup>2</sup> and Thomas M. Truskett<sup>3</sup>

<sup>1</sup>*Department of Chemical Engineering, The University of Texas at Austin, Austin, Texas 78712, USA*

<sup>2</sup>*Department of Chemical and Biological Engineering, University at Buffalo, The State University of New York, Buffalo, New York 14260, USA*

<sup>3</sup>*Department of Chemical Engineering and Institute for Theoretical Chemistry, The University of Texas at Austin, Austin, Texas 78712, USA\**

(Received 21 December 2007; published 14 March 2008)

Density profiles are the most common measure of inhomogeneous structure in confined fluids, but their connection to transport coefficients is poorly understood. We explore via simulation how tuning particle-wall interactions to flatten or enhance the particle layering of a model confined fluid impacts its self-diffusivity, viscosity, and entropy. Interestingly, interactions that eliminate particle layering significantly reduce confined fluid mobility, whereas those that enhance layering can have the opposite effect. Excess entropy helps to understand and predict these trends.

DOI: [10.1103/PhysRevLett.100.106001](https://doi.org/10.1103/PhysRevLett.100.106001)

PACS numbers: 83.10.Rs, 61.20.Ja, 65.40.G–, 66.10.C–

Particles of confined fluids structure in an inhomogeneous manner. As a result, their relaxation processes occur at different rates than in the bulk. Although density profiles of confined fluids can be predicted by classical density functional theory (DFT), a fundamental microscopic framework for predicting transport coefficients has yet to emerge. In fact, even an intuitive understanding of how the density profile connects to dynamics is lacking.

For bulk fluids, semiempirical structure-property relations have helped to correlate and predict transport coefficients (see, e.g., [1–3]). Specifically, changes in thermodynamic state variables that increase short-range structural order of fluids are also known to decrease their mobility in a simple, quantifiable way. This is true even for systems that exhibit anomalous dynamical behavior, such as cold liquid water (where viscosity decreases upon compression) [4–6] or concentrated colloidal suspensions (where interparticle attractions increase mobility) [5,7]. Naïve extrapolation of this idea might lead one to suspect that inhomogeneous fluids with highly structured (e.g., layered) density profiles would tend to be more viscous and less diffusive than more spatially uniform fluids. Is that indeed the case? Here, we explore this issue quantitatively. Specifically, we use molecular simulation to investigate the relationship between the transport coefficients of an inhomogeneous fluid and its density profile, the latter of which can be modified in a precise way through the interactions of the fluid particles with the confining boundaries.

A key empirical observation motivating this study is the existence of an isothermal correlation between the self-diffusion coefficient of simple inhomogeneous fluids and excess entropy (relative to ideal gas), which is approximately obeyed across a wide range of confining environments [8–10]. Since the magnitude of the excess entropy is itself a measure of structural order [11], the aforementioned correlation is effectively a structure-property relationship. But how does excess entropy connect to the

density profile? Do fluids with more structured density profiles generally have lower or higher values of excess entropy when compared to spatially uniform fluids? Moreover, can excess entropy be tuned via the fluid-boundary interactions to modify the transport coefficients in a controlled and predictable way? If so, this idea might be used to great effect in the engineering of micro- and nanofluidic systems.

To address these open questions, we turn to the Weeks-Chandler-Andersen (WCA) model [12], which is known to capture the entropic packing effects that control many properties of dense, atomistic, and colloidal fluids. The WCA pair potential is defined as  $\phi(r) = 4\epsilon([\sigma/r]^{12} - [\sigma/r]^6) + \epsilon$  for  $r < 2^{1/6}\sigma$  and  $\phi(r) = 0$  for  $r > 2^{1/6}\sigma$ , where  $r$  is the interparticle separation. We consider this fluid confined to a thin film geometry between two parallel, planar boundaries placed a distance  $H$  apart. Particles located a distance  $z$  from one boundary ( $0 < z < H$ ) interact with an external field  $\phi_{\text{ext}}(z) = \phi_{\text{fw}}(z) + \phi_{\text{fw}}(H - z)$ . The single-wall potential is given by  $\phi_{\text{fw}}(z) = (2/15) \times [\sigma/z]^9 - [\sigma/z]^3 + \sqrt{10}\epsilon/3 + \phi_0(z)$  for  $z < (2/5)^{1/6}\sigma$  and  $\phi_{\text{fw}}(z) = \phi_0(z)$  for  $z > (2/5)^{1/6}\sigma$ . This represents a WCA 9–3 repulsive boundary plus an additional term  $\phi_0(z)$ , which can be used to tune the density profile. From here forward, we simplify notation by reporting quantities implicitly nondimensionalized by appropriate combinations of the characteristic length scale  $\sigma$  and energy scale  $\epsilon$  (or equivalently  $k_B T$ , since we set  $\epsilon = k_B T$  for all calculations). In the above,  $k_B$  is the Boltzmann constant and  $T$  is temperature.

Our aim is to investigate, for given values of film thickness  $H$  and average fluid density  $\rho_{\text{avg}} = H^{-1} \int_0^H \rho(z) dz$ , how the details of the density profile  $\rho(z)$  impact relaxation processes. This can be done systematically if a suitable set of target density profiles can be chosen for study. For fixed chemical potential  $\mu$ ,  $H$ , and  $T$ , there is a one-to-one

mapping between  $\phi_0(z)$  and  $\rho(z)$  [13]. In fact, as explained below, the specific  $\phi_0(z)$  that will produce a given target density profile can be determined precisely using Monte Carlo (MC) simulation methods. Once determined,  $\phi_0(z)$  can then be imposed in an equilibrium molecular dynamics simulation to calculate the transport coefficients of the fluid.

The baseline density profile that we consider is the “natural” one for the WCA fluid confined between WCA 9–3 walls, i.e., the profile adopted by the equilibrium fluid when  $\phi_0(z) = 0$ . It is characterized by a moderately inhomogeneous structure of fluid particles layered parallel to the confining boundaries.

A second type of profile we consider is a “flat” density distribution, where the layered structure of the confined WCA fluid is effectively eliminated by judicious choice of  $\phi_0(z)$ . We define this flat profile to be equivalent to that which an equilibrium fluid of noninteracting particles with average density  $\rho_{\text{avg}}$  would adopt in the presence of the boundary potential  $\phi_{\text{ext}}(z)$  with  $\phi_0(z) = 0$ . Figure 1(a) compares the shapes of typical flat and natural density profiles, and Fig. 1(c) shows the external potentials  $\phi_{\text{ext}}(z)$  that produce them. Interestingly, because of the nonlocal coupling of  $\phi_{\text{ext}}(z)$  to  $\rho(z)$ , the layering structure of WCA particles in the natural profile can be generally eliminated by the addition of a nonoscillatory, repulsive contribution to the external field. As we demonstrate below, flattening the density profile in this way has the effect of reducing both the entropy and the excess entropy of the confined fluid.

Alternatively,  $\phi_0(z)$  can be chosen such that the confined fluid takes on a higher excess entropy (and, thus, perhaps a higher mobility) than when  $\phi_0 = 0$  (i.e., the natural density profile). To demonstrate this, we investigate a third class of density distributions that we refer to as “structured.” The procedure for generating structured density profiles is described in detail elsewhere [14]. In short,

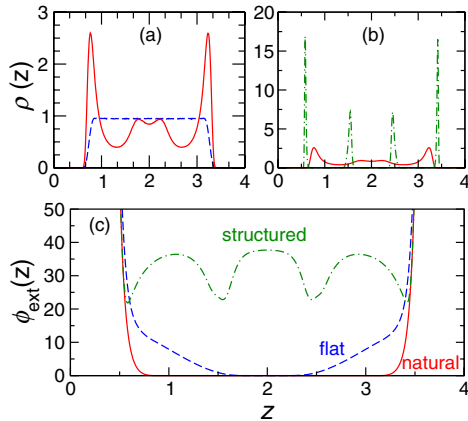


FIG. 1 (color online). (a) Natural and flat density profiles  $\rho(z)$ , and (b) natural and structured density profiles for a confined WCA fluid with average density  $\rho_{\text{avg}} = 0.6$  and  $H = 4$ , as discussed in the text. (c) The associated particle-boundary interactions  $\phi_{\text{ext}}(z)$ .

they correspond to confined fluid states predicted by an approximate DFT to have particularly high values of excess entropy. As is evident in Fig. 1(b), structured profiles do have more pronounced layering than their natural counterparts, an *a posteriori* justification for their name. Moreover, the MC simulations described below verify that they indeed correspond to states with higher excess entropy (but lower entropy) than those with the natural profile.

Here, excess entropy is defined in the usual way as the difference between the fluid’s entropy and that of an ideal gas with the same density profile. To obtain excess entropy data for the aforementioned systems, we employed a suite of MC techniques. First, we used grand canonical transition matrix MC simulations [15] with volume  $V = 1000$  to determine excess entropy as a function of  $N$  and  $H$  for the natural profile case. A detailed explanation of this approach can be found in [4,8]. For select values of  $N$  and  $H$ , we then determined the  $\phi_0(z)$  that generated a target (flat or structured) density profile. We subsequently used an expanded ensemble MC [16] procedure to determine the excess entropy of a fluid subjected to this potential.

To compute  $\phi_0(z)$ , we used an efficient nonequilibrium MC potential refinement technique recently introduced by Wilding [17]. The potential was initialized with  $\phi_0(z) = 0$  and subsequently tuned during an eight-stage canonical MC simulation. At regular intervals during the  $i$ th stage,  $\phi_0(z)$  was incremented by the relative difference between the instantaneous and target density profiles scaled by a modification factor  $y_i = 0.001/2^i$ . Each stage terminated when  $\zeta$ , the maximum relative difference between the target and aggregated stage density profiles, dropped below a tolerance of  $\zeta^* = 0.01$ .

Thermodynamic properties of the confined WCA fluid subjected to a nonzero target  $\phi_0(z)$  were determined through canonical expanded ensemble simulations [16]. A system with a flat or structured profile was related to that with a natural profile through a series of subensembles in which the target potential  $\phi_0(z)$  was scaled by a factor  $\lambda$  that spanned from 0.0 to 1.0 in increments of 0.001. A transition matrix MC technique similar to that described in [18] was used to determine the relative Helmholtz free energy  $F(\lambda)$  of each subensemble. The average energy  $E(\lambda)$  was also accumulated during a simulation. The total entropy difference  $\Delta S(\lambda) = S(\lambda) - S(0)$  between a subensemble characterized by  $\lambda$  and a fluid with a natural profile was evaluated as  $\Delta S(\lambda) = T^{-1}([E(\lambda) - E(0)] - [F(\lambda) - F(0)])$ . The corresponding difference in the excess entropy  $\Delta S^{\text{ex}}(\lambda)$  can be written as  $\Delta S^{\text{ex}}(\lambda) = \Delta S(\lambda) - \Delta S^{\text{id}}(\lambda)$ . The term  $\Delta S^{\text{id}}(\lambda) = -VH^{-1} \int_0^H [\rho(z, \lambda) \times \ln \rho(z, \lambda) - \rho(z, 0) \ln \rho(z, 0)] dz$  is simply the change in entropy of an ideal gas upon changing its density profile from  $\rho(z, 0)$  to  $\rho(z, \lambda)$ .

We computed the transport coefficients of the thin films via molecular dynamics simulations in the microcanonical ensemble using  $N = 4000$  particles and integrating the

equations of motion with the velocity-Verlet algorithm [19]. A time step of 0.0025 was used for simulating the natural and flat profile systems, while a shorter time step of 0.0002 was employed for the structured profile fluids. Periodic boundary conditions were employed in the  $x$  and  $y$  “free” directions. We extracted values of self-diffusivity (parallel to the walls)  $D$  by fitting the long-time ( $t \gg 1$ ) behavior of the mean-squared displacement to the Einstein relation for diffusion  $\langle \Delta \mathbf{r}^2 \rangle = 4Dt$ , where  $\langle \Delta \mathbf{r}^2 \rangle$  represents the mean-squared displacement in the  $x$  and  $y$  directions. Similarly, we calculated values of zero-shear viscosity  $\eta$  from the long-time behavior of  $\langle \Delta A^2 \rangle$  via its corresponding Einstein relation,  $\langle \Delta A^2 \rangle = 2\eta Tt/V$ . Here,  $\Delta A = \int_0^t \sigma_{xy}(\tau) d\tau$  is the time integral of the  $xy$  component of the stress tensor.

To systematically probe the effects of flattening or enhancing the layering of the density profile, we first focus on the behavior of the confined fluid for  $\rho_{\text{avg}} = 0.6$  and  $H = 4$ . Let  $\phi_{0,f}(z)$  and  $\phi_{0,s}(z)$  represent the contributions to the external potential that, under these conditions, produce the flat and structured profiles, respectively. Starting from the natural profile, we incrementally flatten the density distribution by choosing  $\phi_0(z) = \lambda_f \phi_{0,f}(z)$  with progressively larger values of  $\lambda_f$  in the range  $0 \leq \lambda_f \leq 1$ . Similarly, we systematically enhance the layering of the natural profile by setting  $\phi_0(z) = \lambda_s \phi_{0,s}(z)$  with progressively larger values of  $\lambda_s$  in the range  $0 \leq \lambda_s \leq 1$ .

In Fig. 2, we show how these specific ways of modifying the density distribution in turn affect the entropy per particle  $s$ , the excess entropy per particle  $s^{\text{ex}}$ , the self-diffusivity  $D$ , and the viscosity  $\eta$ . As expected,  $s$  appears highest for the natural profile. This is because the system is virtually athermal when  $\phi_0 = 0$  due to the steep boundary and interparticle repulsions. As a result, its equilibrium (minimum free energy) structure also approximately maximizes  $s$  relative to other fluid states [i.e., other  $\phi_0(z)$  and corresponding density profiles] with the same  $\rho_{\text{avg}}$  and  $H$ . The natural profile state does not, however, maximize  $s^{\text{ex}}$ . Rather,  $s^{\text{ex}}$  is found to monotonically increase with increased “structuring” of the density profile. How can we understand these trends?

The key is to recall that  $\Delta s^{\text{id}}(\lambda) = \Delta s(\lambda) - \Delta s^{\text{ex}}(\lambda)$  quantifies how changing  $\lambda$  and, in turn, the density profile modifies the ideal gas entropy, while  $\Delta s^{\text{ex}}(\lambda)$  measures the corresponding entropic change associated with the interacting fluid’s interparticle correlations. With this in mind, it is clear that flattening the natural profile will inevitably result in an increase in ideal gas entropy [i.e.,  $\Delta s^{\text{id}}(\lambda_f) > 0$ ]. Moreover, since  $s$  generally decreases upon flattening of the natural profile, it follows that  $s^{\text{ex}}$  will also generally decrease, reflecting an overall strengthening of interparticle correlations. In other words, paradoxically, the fluid with the flat density profile exhibits the highest degree of structural order.

On the other hand, it is also self-evident that enhancing the layering of the natural density profile will decrease the

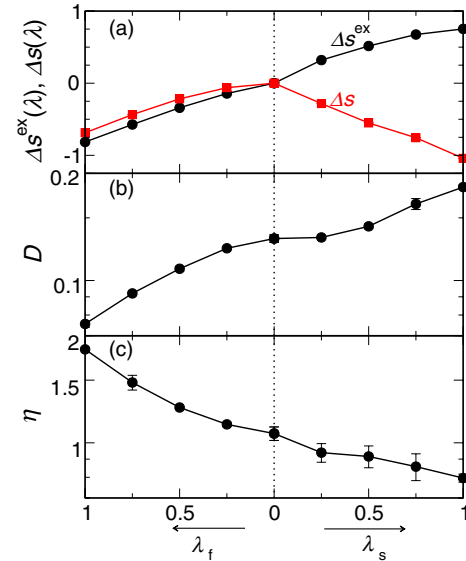


FIG. 2 (color online). Effect of boundary interaction (shape of density profile) on (a) excess entropy per particle  $\Delta s^{\text{ex}}(\lambda) = s^{\text{ex}}(\lambda) - s^{\text{ex}}(0)$  and entropy per particle  $\Delta s(\lambda) = s(\lambda) - s(0)$ , (b) self-diffusivity  $D$ , and (c) viscosity  $\eta$  for the confined WCA fluid with  $\rho_{\text{avg}} = 0.6$  and  $H = 4$ . The center line corresponds to the fluid with the natural density profile of Figs. 1(a) and 1(b). From center to left, the density profile is systematically flattened:  $\phi_0(z) = \lambda_f \phi_{0,f}(z)$ , where  $\lambda_f = 1$  yields the flat profile shown in Fig. 1(a). From center to right, the density profile is structured:  $\phi_0(z) = \lambda_s \phi_{0,s}(z)$ , where  $\lambda_s = 1$  produces the structured profile shown in Fig. 1(b). Symbols are simulation data, and curves are guides to the eye.

ideal gas entropy [i.e.,  $\Delta s^{\text{id}}(\lambda_s) < 0$ ]. Since  $s$  also decreases in this process, the aforementioned entropic penalty can at most be partially compensated by an increase in  $s^{\text{ex}}$  due to diminished interparticle correlations. In fact, Fig. 2 provides a specific example for how structuring the density profile can significantly decrease the overall structural order (i.e., increase  $s^{\text{ex}}$ ) of the confined fluid. One should keep in mind that the specific structured profiles examined here were selected precisely because DFT predicted that they would have high values of  $s^{\text{ex}}$ . Thus, we emphasize that while flattening the natural density profile can generally be expected to decrease  $s^{\text{ex}}$ , alternative means for embellishing its structure at constant  $\rho_{\text{avg}}$  may either increase or decrease  $s^{\text{ex}}$ . The case studied here provides proof of concept for the former. We will extensively discuss the latter case in a future publication.

A second important point of Fig. 2 is that the mobility of the confined fluid, as measured by both  $\eta^{-1}$  and  $D$ , closely tracks the behavior of  $s^{\text{ex}}$  (but not  $s$ ) for the flattening and structuring processes described above. A physical explanation is that fluid transport parallel to the walls is dominated by interparticle collisions, and hence structural correlations [1–3]. The density profile appears to impact these transport processes mostly due to the fact that it modifies the interparticle correlations, the effect of which

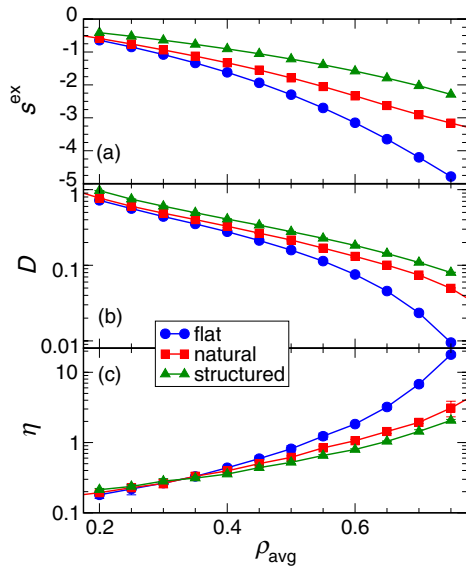


FIG. 3 (color online). (a) Excess entropy per particle  $s^{\text{ex}}$ , (b) self-diffusivity  $D$ , and (c) viscosity  $\eta$ , of the confined WCA fluid versus average density  $\rho_{\text{avg}}$  at  $H = 4$ . Symbols are simulation data, and curves are guides to the eye.

is conveniently isolated by computing the excess rather than the total entropy of the fluid.

The above observation that fluids with more uniform density profiles can actually have lower  $s^{\text{ex}}$  and slower dynamics than those with strongly layered density profiles (and the same  $\rho_{\text{avg}}$ ) appears even more general when viewed in the context of other recent simulation data. In particular, it is now known that the hard-sphere fluid confined between hard walls shows lower  $s^{\text{ex}}$  [9] and slower single-particle dynamics both parallel [9] and normal [20] to the confining walls when such walls are separated by distances that inherently frustrate the ability of the fluid to structure into an integer number of layers in its density profile. These model predictions of the relationship between dynamics and density profiles can now also be tested in experiments, e.g., by using confocal microscopy to investigate confined “hard-sphere” colloidal suspensions [21].

To document the generality of the physics discussed above, we show in Fig. 3 the behaviors of  $s^{\text{ex}}$ ,  $\eta$ , and  $D$  over a broad range of average film densities. Perhaps most striking is the observation that, at high density, fluids with structured and flat density profiles with the same  $\rho_{\text{avg}}$  can differ in both  $D$  and  $\eta$  by an order of magnitude. Although the current study focuses on equilibrium fluid conditions, the trends evident in Fig. 3 suggest that one might even be able to effectively supercool monatomic confined fluids by isothermally modifying the external potential in a way that systematically flattens the density profile. Finally, we note that counterintuitive connections between ordering and dynamics have also been observed in driven systems [22,23]. Whether one can generalize the equilibrium ap-

proach presented here to gain insights into such phenomena (e.g., the shear-induced changes to liquid structure and viscosity [22]), however, remains an open question.

T. M. T., J. R. E., and W. P. K. acknowledge support of the National Science Foundation (Grants No. CTS-0448721, No. CTS-028772, and the NSF graduate program, respectively). T. M. T. also acknowledges support of the David and Lucile Packard Foundation and Alfred P. Sloan Foundation. The Texas Advanced Computing Center and University at Buffalo Center for Computational Research provided computational resources for this study.

\*truskett@che.utexas.edu

- [1] Y. Rosenfeld, Phys. Rev. A **15**, 2545 (1977).
- [2] Y. Rosenfeld, J. Phys. Condens. Matter **11**, 5415 (1999).
- [3] M. Dzugutov, Nature (London) **381**, 137 (1996).
- [4] J. R. Errington, T. M. Truskett, and J. Mittal, J. Chem. Phys. **125**, 244502 (2006).
- [5] J. Mittal, J. R. Errington, and T. M. Truskett, J. Phys. Chem. B **110**, 18147 (2006).
- [6] R. Sharma, S. N. Chakraborty, and C. Chakravarty, J. Chem. Phys. **125**, 204501 (2006).
- [7] W. P. Krekelberg, J. Mittal, V. Ganesan, and T. M. Truskett, J. Chem. Phys. **127**, 044502 (2007).
- [8] J. Mittal, J. R. Errington, and T. M. Truskett, Phys. Rev. Lett. **96**, 177804 (2006).
- [9] J. Mittal, J. R. Errington, and T. M. Truskett, J. Chem. Phys. **126**, 244708 (2007).
- [10] J. Mittal, J. R. Errington, and T. M. Truskett, J. Phys. Chem. B **111**, 10054 (2007).
- [11] T. M. Truskett, S. Torquato, and P. G. Debenedetti, Phys. Rev. E **62**, 993 (2000).
- [12] D. Chandler, J. D. Weeks, and H. C. Andersen, Science **220**, 787 (1983).
- [13] J. D. Weeks, J. Stat. Phys. **110**, 1209 (2003).
- [14] See EPAPS Document No. E-PRLTAO-100-019812 for the protocol for generating high excess entropy structured density profiles. For more information on EPAPS, see <http://www.aip.org/pubservs/epaps.html>.
- [15] J. R. Errington, J. Chem. Phys. **118**, 9915 (2003).
- [16] A. P. Lyubartsev, A. A. Martynov, S. V. Shevkunov, and P. N. Vorontsov-Velyaminov, J. Chem. Phys. **96**, 1776 (1992).
- [17] N. B. Wilding, J. Chem. Phys. **119**, 12163 (2003).
- [18] J. R. Errington and D. A. Kofke, J. Chem. Phys. **127**, 174709 (2007).
- [19] M. P. Allen and D. J. Tildesley, *Computer Simulation of Liquids* (Clarendon Press, New York, 1989).
- [20] J. Mittal, T. M. Truskett, J. R. Errington, and G. Hummer, arXiv:0801.0757v1.
- [21] C. R. Nugent, K. V. Edmond, H. N. Patel, and E. R. Weeks, Phys. Rev. Lett. **99**, 025702 (2007).
- [22] J. J. Erpenbeck, Phys. Rev. Lett. **52**, 1333 (1984).
- [23] D. Helbing, I. J. Farkas, and T. Vicsek, Phys. Rev. Lett. **84**, 1240 (2000).